American Journal of Pathology, Vol. 160, No. 3, March 2002

Thymosin-β4 Regulates Motility and Metastasis of Malignant Mouse Fibrosarcoma Cells

Tokushige Kobayashi,* Futoshi Okada,* Nobuyuki Fujii,† Naoko Tomita,† Satoru Ito,† Hiroshi Tazawa,* Tetsuya Aoyama,§ Sung Ki Choi,* Toshiyuki Shibata,§**¶ Hisakazu Fujita,‡ and Masuo Hosokawa*

From the Division of Cancer Pathobiology, Research Section of Pathophysiology, and the Division of Cancer Gene Regulation,‡ Research Section of Disease Control, Institute for Genetic Medicine, Hokkaido University, Sapporo, Japan; Fujirebio† Incorporated, Diagnostic Research Laboratories, Hachioji, Japan; and the Second Department of Oral and Maxillofacial Surgery,§ Health Sciences University of Hokkaido, Tobetsu, Ishikari,** Oral and Maxillofacial Surgery,¶ Gifu University School of Medicine, Tsukasa, Gifu, Japan*

We identified a thymosin-β4 gene overexpression in malignant mouse fibrosarcoma cells (QRsP-30) that were derived from clonal weakly tumorigenic and nonmetastatic QR-32 cells by using a differential display method. Thymosin-β4 is known as a 4.9-kd polypeptide that interacts with G-actin and functions as a major actin-sequestering protein in cells. All of the six malignant fibrosarcoma cell lines that have been independently converted from QR-32 cells expressed high levels of thymosin-β4 mRNA and its expression in tumor cells was correlated with tumorigenicity and metastatic potential. Up-regulation of thymosin-β4 in QR-32 cells (32-S) transfected with sense thymosin-β4 cDNA converted the cells to develop tumors and formed numerous lung metastases in syngeneic C57BL/6 mice. In contrast, antisense thymosin-β4 cDNA-transfected QRsP-30 (30-AS) cells reduced thymosin-β4 expression, and significantly lost tumor formation and metastases to distant organs. Vector-alone transfected cells (32-V or 30-V cells) behaved like their parental cells. We observed that tumor cell motility, cell shape, and F-actin organization is regulated in proportion to the level of thymosin-β4 expression. These findings indicate that thymosin-β4 molecule regulates fibrosarcoma cell tumorigenicity and metastasis through actin-based cytoskeletal organization. ***(Am J Pathol , :869–882)***

Tumor development and progression occur in a consecutive and multistep process that involves several gene alterations. The most serious change is the latter process, tumor progression, because tumor cells acquire an invasive and metastatic phenotype that is the main cause of death and a major barrier to successful treatment for cancer patients. Therefore, for early diagnosis and effective therapeutic intervention, we need to detect the alterations associated with transition from benign to malignant tumor cells on a molecular basis.

Animal tumor models are revealing genes associated with tumor progression that also appear in human cancers such as NM23,[1] Kiss-1,[2] mts1,[3] and CD44,[4] which are differentially expressed between high- and low-metastatic tumor cells. The tumor progression model of mouse fibrosarcoma cells (QR clone) has been established by our group, which has advantages compared to other models.[5–10] The QR tumor clones regress spontaneously after injection of up to 2×10^5 cells subcutaneously or 1×10^6 cells intravenously in normal syngeneic mice; the tumor regression is mediated by host immunity because the tumor cells grow progressively in immunosuppressed or nude mice and a tumor cell-derived immunosuppressive factor, prostaglandin E_2 (PGE_2) is associated with this process.[11] Thus by using QR clones, we are able to mimic the natural course of tumor progression, ie, transition from weak tumorigenicity and nonmetastatic benign tumor cells or dormant state of tumor cells to tumorigenic/metastatic malignant tumor cells in mice. The transitional change can be determined by augmented tumorigenicity or metastatic potential.[5–10] The model is available for detection of possible internal or external factors for tumor progression. We have previously identified that inflammation[5–7,12] or antitumor drug treatments[8–10] accelerated tumor progression and the resultant daughter cells possessed irreversibly stable malignant phenotypes, all of which derived from a clonal QR-32 tumor line. Comparison of the genes between single-cell-originated benign tumor cells and its derived malignant tumor cells would be of benefit for identifying the progression-associated gene alterations because of their very close genetic backgrounds.

We tried to define gene expression comparatively between QR-32 cells and its derived progressor cell line, QRsP-30 cells by differential display and the identified

Supported in part by a grant-in-aid for Cancer Research from the Japanese Ministry of Health, Labor, and Welfare (10-1 to M. H. and 10-36 to F. O.) and a grant-in-aid from Japanese Ministry of Education, Culture, Sports, Science, and Technology (to F. O.).

Accepted for publication November 21, 2001.

Address reprint requests to Futoshi Okada, Ph.D., Division of Cancer Pathobiology, Research Section of Pathophysiology, Institute for Genetic Medicine, Hokkaido University, Kita-15, Nishi-7, Kita-ku, Sapporo, 060-0815, Japan. E-mail: fuokada@med.hokudai.ac.jp.

thymosin-β4 gene was transcriptionally elevated in all of the malignant tumor cell lines we tested. We demonstrated that thymosin-β4 expression regulated tumorigenicity, cell motility, and metastatic potential of fibrosarcoma cells through actin-based cytoskeletal organization by sense and antisense thymosin-β4 cDNA transfection strategy.

Materials and Methods

Cell Lines and Culture Conditions

The weakly tumorigenic and poorly metastatic mouse clonal fibrosarcoma cell line QR-32, its derivative highly tumorigenic and highly metastatic cell line, QRsP, and the transfectants were maintained as previously described.[5,7] Briefly, these cell lines were maintained in Eagle's minimum essential medium that contained 8% fetal bovine serum, sodium pyruvate, nonessential amino acids and L-glutamine, at 37°C, in a humidified 5% carbon dioxide/95% air mixture.

mRNA Differential Display

The mRNA differential display was performed following the original technique described by Liang and Pardee.[13] DNase I-digested total RNA (1 μg) from QR-32 and QRsP-30 cells were, respectively, reverse-transcribed with 200 U of Superscript RNase H-reverse transcriptase (GIBCO BRL) in the presence of 2.5 μmol/L of one of four anchored primers, T_{15}MG, T_{15}MC, T_{15}MA, and T_{15}MT (Operon Technologies Inc.). Sixty arbitrary 10-mer primer (Operon Technologies, Inc.) was selected at random to be used for polymerase chain reaction (PCR) with the appropriate anchored primer with 5 U/μl of *Taq* polymerase (Takara). The cycling conditions were 3 minutes at 94°C, 5 minutes at 40°C, 5 minutes at 72°C (1 cycle), 15 seconds at 95°C, 2 minutes at 40°C, 1 minute at 72°C (25 cycles), and 5 minutes at 72°C (1 cycle). Two independent reaction products, respectively, from QR-32 and QRsP-30 cells were separated in 8% polyacrylamide gel with glycerol-tolerant running buffer (United States Biochemical). Differentially expressed cDNA bands were directly excised from the gel and reamplified with the same primer sets in high-stringency conditions. Bands were then cloned into pGEM-T (Promega Corp.) and sequenced with ALF express sequencer (Amersham Pharmacia Biotech).

Vector Construction of Sense or Antisense Nucleotide of Thymosin-β4 and Preparation of Transfectants

The coding region of thymosin-β4 (nucleotides 158 to 292) was cloned from QRsP-30 cDNA library by PCR. The coding region of thymosin-β4 cDNA was inserted into the pcDNA3.1 vector, which contains the cytomegalovirus enhancer-promoter (Invitrogen) at the *Pme*I and *Xho*I sites in the direction of sense or antisense orientation. The orientation of the insert was determined by enzymatic digestion and it was confirmed that no mutations were introduced during the PCR amplification by direct DNA sequencing (data not shown).

The thymosin-β4 sense or antisense vector, and the vector alone pcDNA3.1 were individually transfected into tumor cells with Lipofectin reagent (GIBCO/BRL). Transfectants stably expressing the introduced vector were selected by continuous neomycin treatment with 400 μg/ml (Geneticin, GIBCO/BRL). Neomycin-resistant cells were cloned by the limiting dilution method and maintained in the medium containing neomycin.

RNA Extraction and Northern Blot Analysis

Total RNA was isolated from cells exponentially growing *in vitro* with a Trizol reagent (GIBCO/BRL). Twenty μg of total RNA was size-fractionated on a denaturing formaldehyde-agarose gel (1.0%) and transferred onto *trans*-Blot transfer membrane (Bio-Rad). The membrane was hybridized at 42°C for 24 hours with denatured thymosin-β4 probe labeled with [α-^{32}P] dCTP (Amersham) with the use of a random-primer DNA-labeling kit (Takara, Japan) in the buffer containing 50% formamide, 5× SSPE, 0.5% sodium dodecyl sulfate (SDS), 5× Denhardt's solution, and 100 μg of denatured salmon sperm DNA. Then the membranes were washed with 2× standard saline citrate and 0.1% SDS at room temperature for 10 minutes, 0.2× standard saline citrate and 0.1% SDS at room temperature for 10 minutes, and then 0.2× standard saline citrate and 0.1% SDS at 42°C for 60 minutes. To confirm the amounts of RNA loaded in each lane, the blots were hybridized afterward with a L38 cDNA.[14] Image analysis was performed with BAS2000II system (FUJIX, Japan).

Reverse Transcriptase (RT)-PCR Analysis

Three hundred ng of total RNA was used for the synthesis of the first-strand cDNA in a 20-μl reaction mixture containing 1× first-strand buffer (GIBCO/BRL), 7.5 mmol/L dithiothreitol, 0.5 mmol/L $MgCl_2$, 0.5 mmol/L dNTO, 100 pg random primer (GIBCO/BRL), and Moloney murine leukemia virus reverse transcriptase (GIBCO/BRL). The reverse transcription was done in a block incubator (Astec, B1-525; Japan) for 50 minutes at 37°C after annealing at 25°C for 10 minutes. PCR was performed at 95°C for 5 minutes and on ice for 5 minutes in a block incubator. PCR was performed in a 20-μl reaction mixture containing 1× native pfu buffer (Stratagene), 200 nmol/L of each primer, 0.2 mmol/L dNTPs, and 0.25 U of native pfu polymerase (Stratagene). Gene-specific primers were designated to span the coding region of mouse thymosin-β4 (5′ to 3′); thymosin-β4 upstream, CCTCATCCTCCTCGTCCTTA; thymosin-β4 downstream, TGATCCAACCTCTTTGCATC. Control studies for RT-PCR were conducted by using aliquots from the same samples and amplifying them with primers to GAPDH gene (5′ to 3′); mouse GAPDH upstream, GGGTGTGAACCACGAGAAAT; mouse GAPDH downstream,

GGTCCTCAGTGTAGCCCAAG. RT-PCR of mRNA encoding mouse thymosin-β4 and GAPDH resulted in PCR products of 295- and 442-bp long, respectively. The PCR cycles consisted of 1 minute initial denaturation at 95°C, followed by 35 cycles of 95°C for 40 seconds, 59°C for 40 seconds, and 78°C for 1.5 minutes in a thermal cycler (2400R, Perkin Elmer). Each PCR amplification included a negative control containing all of the reaction products except cDNA. Five μl of each PCR product was separated in 2% agarose (Iwai Chem. Pharm., Japan), and stained with ethidium bromide, and photographed under UV light.

Thymosin-β4 Monoclonal Antibody Preparation and Peptide Inhibition Assay

Because synthetic full-size peptide of human thymosin-β4 gave no antibody rise on intraperitoneal injections into BALB/c mice, we therefore used the N-terminal half of thymosin-β4 molecule. The synthetic peptide (Thyb4-2: MSDKPDMAEIEKFDKSKLKKTETQEKN) was made with an additional Cys moiety at the C-terminal position for conjugation with KLH. Mice were immunized three times with the Thyb4-2 (20 μg/ml) and Freund's complete adjuvant. Two weeks later, the mice were boosted with Thyb4-2 and Freund's noncomplete adjuvant. After the final immunization, the spleen was fused with myeloma cells (P3U1) and 50% PEG (1500; Boehringer Mannheim Yamanouchi, Tokyo, Japan) with the standard screening method to obtain a desired monoclonal antibody, TB4N1-5. The subclass of the antibody was IgG1 (κ). The established hybridoma cells were injected intraperitoneally into BALB/c mice to produce ascites and the antibody was purified with the use of a protein-A column.

For peptide competitive inhibition assay, 96-well plates were coated with synthetic peptide Tyb4-2 (2 μg/ml) of thymosin-β4 for overnight at 4°C. After washing with phosphate-buffered saline (PBS) containing 0.02% Tween 20 (T-PBS), the plates were incubated with 1% skim milk in PBS. Then TB4N1-5 antibody (5 μg/ml) was added to the wells with serially diluted synthetic peptide Tyb4-2 (for thymosin-β4) or Tyb10 (for thymosin-β10, full size) as a control, and the plates were incubated for 3 hours at 37°C. After three washes, anti-mouse immunoglobulins conjugated with horseradish peroxidase were added to the wells and incubated for 1 hour at 37°C. After three washes, an ABTS [2,2′-azino-bis(3-ethylbenzthiazoline-6-sulfonic acid) diammonium salt]/H_2O_2 solution (0.1%/0.003%) in citrate/phosphate buffer (0.1 mol/L, pH 4.5) was added to each well. After 10 minutes, absorbance was measured at 405 nm.

Protein Extraction and Western Blotting

Proteins were extracted from cell lines and Western blot analysis was performed as follows. Briefly, lysates of the cultured cells were prepared in Laemmli's buffer.[15] Then 100 μg of the protein was separated by electrophoresis on a SDS-10% polyacrylamide gel. The gel was incubated in phosphate-buffered saline (PBS) containing 10% glutaraldehyde (Wako Pure Chemical Ind., Japan) for 1 hour, washed three times in PBS for 20 minutes, and further incubated in a blotting buffer for 30 minutes at room temperature. The protein was transferred to a polyvinylidene difluoride membrane (Immobilon-P; Millipore, Japan) by electrotransfer. The membrane was preincubated for 2 hours with 5% skim milk in PBS containing 0.05% T-PBS. The membrane was incubated for 1 hour at room temperature with a monoclonal antibody to thymosin-β4 (TB4N1-5). After five washes with T-PBS, the membrane was incubated with horseradish peroxidase-conjugated sheep anti-mouse immunoglobulin antibody (NA931, Amersham) for 1 hour at room temperature. After five washes of the membrane with T-PBS, the specific protein-antibody reaction was detected by the enhanced chemiluminescence detection system (Amersham). The intensities of individual bands were semiquantified by means of densitometry of autoradiogram with the Kodak Digital Science (IS 440CF). Each membrane was stained with 0.1% Amido Black 10B (161-0402, BioRad) and equivalence of the loading protein was confirmed in each lane.

Immunofluorescence, Texas Red-X Phalloidin Staining, and Confocal Images

Cells from each cell line were allowed to spread on glass coverslips (22 × 22 mm; Matsunami Glass, Japan) in 6-well plates (no. 3046; Falcon). The cells were fixed with 3.0% paraformaldehyde and then permeabilized with 0.1% Triton X-100 for 5 minutes. The cells were treated with 70% methanol for 5 minutes at −30°C and washed with 0.1% bovine serum albumin in T-PBS (PBT). Then the cells were stained with anti-thymosin-β4 antibody (TB4N1-5, 1 μg/ml) for 1 hour, followed by incubation for 1 hour with Alexa 488 anti-mouse IgG (A-11029, 10 μg/ml; Molecular Probes). Thereafter F-actin staining was done by incubating with 1 U of Texas Red-X phalloidin (T-7471, Molecular Probes) for 1 hour. Cells were mounted and analyzed by confocal microscopy as follows. The confocal scanning laser microscope images were generated on a confocal laser-scanning microscope equipped with an argon laser and ZEISS 63× oil immersion (1.4 n.a.) objective. The condition for confocal imaging was fixed as follows and scanning was done exactly and the same condition at one time. Image collection: speed, normal; collection filter, Kalman, Factor 1; and box and pixel size, 512 × 512 pixels (0.4 μm/pixel). PhotoMultiplier: iris, 2.0; gain, 1500; BLev, 0; emission filter, 605 DF32; and low signal, checked. The final images were volume rendered on a computer (DELL Power Edge 2200) using Bio-Rad Sharp Confocal System (MRC-1024 version 3.2, Bio-Rad). The digital images were subsequently photographed with a digitalized film recorder (Color Video Copy Processor, CP2000; Mitsubishi, Japan) onto a paper sheet (model CK2000L, Mitsubishi Electric).

Determination of in Vitro *Tumor Cell Growth, Plating Efficiency, and Soft Agar Colony Formation*

For *in vitro* cell growth analysis, cells were seeded into a 6-well plate (1 × 10^5 cells per well). The medium was

changed every other day. The cells were harvested and counted every day from day 1 to 7 by trypan blue exclusion test. Doubling time was calculated from the logarithmic phase of the growth curve.

For evaluation of plating efficiency, 1×10^3 cells suspended in the medium containing 8% fetal bovine serum were plated into 60-mm dishes (MS-10600; S.B. Medical, Japan) in triplicate. The dishes were incubated for 7 days, and colonies were fixed in Carnoy's fixative, stained with 0.1% crystal violet, and scored.

For determination of the soft agar growth (anchorage-independent), 2×10^2 cells were suspended in 1 ml of the medium containing 0.3% agar (GIBCO/BRL) and twice volume of fetal bovine serum, and applied onto the presolidified 0.6% agar (1 ml) in 6-well plates. Triplicate plates were prepared for each cell line. After 3 weeks of incubation, colonies larger than 0.1 mm in diameter were scored.

In Vitro *Cell Motility Assays*

Phagokinetic Track Assay

Uniform carpets of gold particles were prepared on glass coverslips (22 × 22 mm) coated with bovine serum albumin as described previously.[16] The gold particle on glass coverslips was placed in 35-mm culture dishes (627160, Greiner Labortechnik) containing 2 ml of Eagle's minimum essential medium supplemented with 8% fetal bovine serum. Then 2×10^3 cells were added to each dish. After 48 hours, phagokinetic tracks of 40 cells were visualized under a microscope. The area cleared of gold particles by a cell was quantified by using a microscope analyzer (Cosmozone R500; Nikon, Japan).

Scratch Wound Closure Assay

Confluent tumor-cell monolayers on glass coverslips (22 × 22 mm) in six-well plates were scraped using a pipette tip (MARS, CL-200; Japan) to make a wound 22-mm long. The cells were incubated at 37°C and allowed to migrate into the wound for intervals of several hour, then fixed and stained with 0.1% crystal violet. The numbers of cells that moved into the 22-mm^2 area in each line were counted in a microscope.

Subcutaneous Tumorigenicity and Metastasis Assay in Vivo

Animal protocols were approved by the Committee of Institute for Animal Experimentation at the Hokkaido University School of Medicine (no. 9910). Female C57BL/6 mice were purchased from Japan SLC and used at 6 to 10 weeks of age. Subcutaneous tumorigenicity was examined by injecting 2×10^5 cells/0.2 ml into the subcutis of the mice. In the study on spontaneous metastasis, moribund mice were sacrificed and the organs were removed, weighed, and the number of metastatic nodules on the surface of lung and the other organs were counted macroscopically.

Experimental metastatic potential of the cells was measured by the lung colonization assay as described previously.[5] In brief, the cells were injected into the tail vein of mice at the density of 1×10^6 cells/0.2 ml. Twenty-five days later, the mice were sacrificed and the metastatic nodules on the lung surface and the other organs were counted macroscopically.

Statistical Analysis

Differences in the subcutaneous tumor and those in spontaneous and experimental metastases were evaluated by chi-square test. Differences in the plating efficiency, the latency periods, the mean survival times, and the motility of tumor cells were calculated by Student's *t*-test.

Results

Overexpression of Thymosin-β4 mRNA in Malignant Fibrosarcoma Cell Lines

We have previously found that foreign body-induced inflammation not only promotes the local growth of weakly tumorigenic and nonmetastatic tumor cells (QR-32) but also converts them into more aggressive tumors (QRsP), ie, they acquire enhanced tumorigenicity and metastatic ability.[5] Using differential display, we identified 23 genes that were expressed differentially between QR-32 cells and its derivative highly tumorigenic and metastatic fibrosarcoma cell line, QRsP-30. Based on Northern blot analysis of those 23 genes, we further selected 3 genes. To identify these genes, we extracted the differential display bands, reamplified, and sequenced. A search in the BLAST computer database found that these cDNAs were more than 90% homologous to calcyclin, thymosin-β4, and vimentin, respectively (data not shown). Figure 1 illustrates a typical example of differential display (Figure 1A) and a Northern blot (Figure 1B) that confirms the existence of 0.7-kb thymosin-β4 mRNA in the QRsP-30 cells but not in the parental QR-32 cells.

Northern blot analysis showed that QR-32 cells expressed an extremely low level of thymosin-β4 mRNA (Figure 1, C and D). We observed high levels of thymosin-β4 mRNA expression in a total of five QR-32 cell-derived highly metastatic tumor cell lines (43- to 70-fold; Figure 1, C and D) and relatively high expression of thymosin-β4 mRNA in the moderately metastatic tumor cell line, QRsP-28 (19-fold; Figure 1, C and D). On the other hand, expression of calcyclin and vimentin was observed equally in QR-32 cells and its derived malignant tumor cell lines (data not shown). Thus thymosin-β4 expression was well correlated with malignant phenotype of tumor cells.

Regulation of Thymosin-β4 Expression in QR-32 or QRsP-30 Cells by Sense or Antisense Thymosin-β4 cDNA Transfection

To elucidate the role of thymosin-β4 in tumor malignancy, we introduced the pcDNA3.1 expression vector containing the cDNAs encoding either sense and antisense ori-

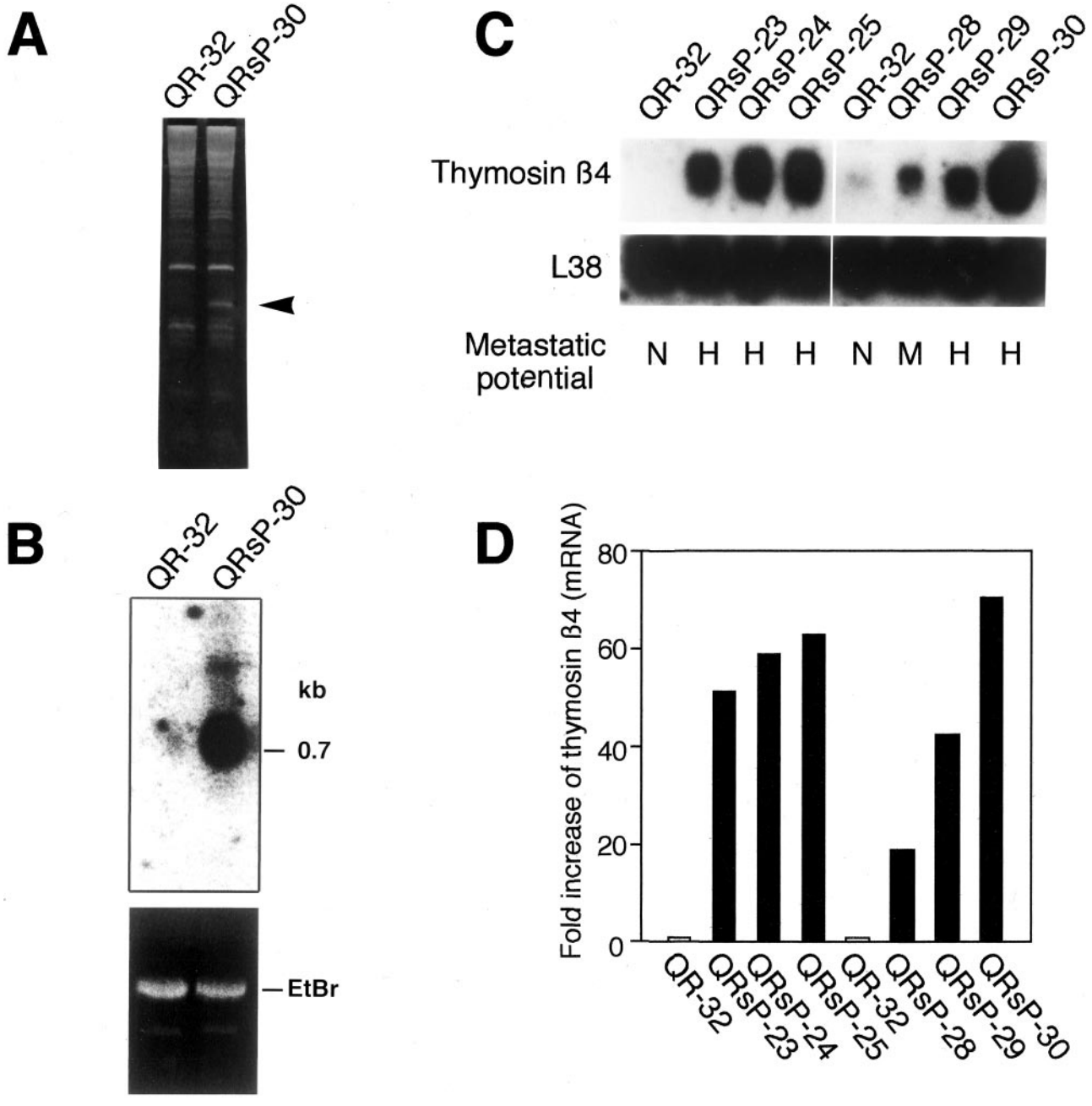

Figure 1. Differential display and Northern blot reveal increased expression of thymosin-β4 in malignant mouse fibrosarcoma cell lines as compared to parental QR-32 cells. **A:** Differential display demonstrates markedly augmented expression of thymosin-β4 (**arrowhead**) in malignant fibrosarcoma cells, QRsP-30 when compared with the parental QR-32 cells. **B:** Northern blot using thymosin-β4 gene as probe identifies a 0.7-kb mRNA expression in QRsP-30 cells (**top**). 28S rRNA expression served as a loading control (**bottom**). **C:** Northern blot confirmed that the expression of thymosin-β4 gene was enhanced in malignant tumor cell lines. L38 hybridization served as a loading control. Metastatic potential of the intravenously injected tumor cells (as described in Materials and Methods). N, nonmetastatic; M, moderately metastatic (forming metastatic colonies not exceeding 150 per lung); H, highly metastatic (forming colonies more than 150 per lung). **D:** The expression of the thymosin-β4 mRNA comparing L38 mRNA were quantified by densitometry.

entation of the mouse thymosin-β4 into QR-32 cells and QRsP-30 cells, respectively. To obtain sense thymosin-β4-transfected QR-32 cells, we initially isolated 24 neomycin-resistant clones, all of which were then screened for expression of thymosin-β4 mRNA. Sense or antisense transcripts of the thymosin-β4 in the transfected cells were determined by RT-PCR amplification with the primers designated to span the coding region of thymosin-β4. Thymosin-β4 was expressed at 295 bp in 32-S cells (Figure 2A). To obtain antisense thymosin-β4-transfected QR-30 cells, we isolated 20 neomycin-resistant clones and then screened for thymosin-β4 and measured its expression. We isolated four 30-AS clones that reduced thymosin-β4 transcripts as shown in Figure 2B. We tested more than 100 clones from QR-32 or QRsP-30 cells transfected with empty vector. However, as far as we tested, we could not find any clone that changed thymosin-β4 expression. Therefore, we considered that alteration of

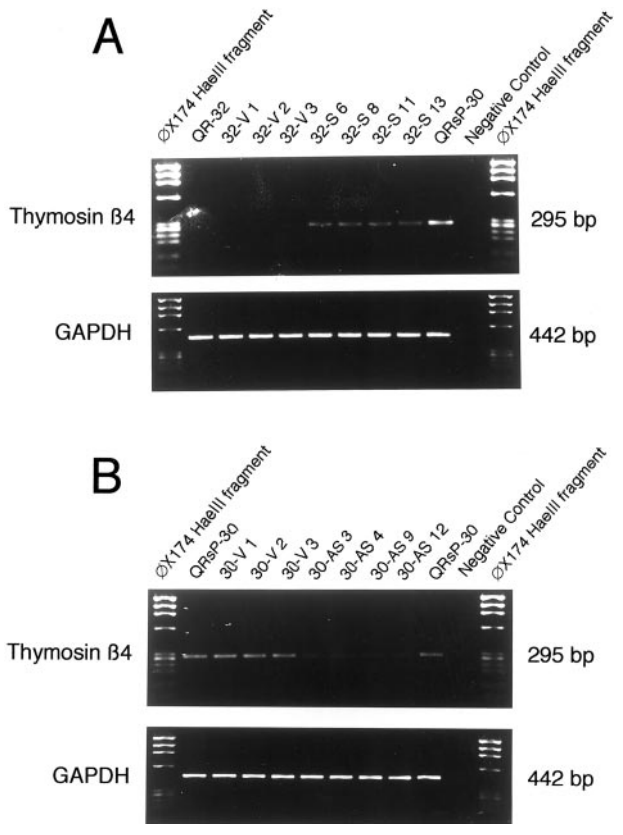

Figure 2. RT-PCR analysis of thymosin-β4 expression in the cells transfected with sense or antisense thymosin-β4 construct and vector controls. RT-PCR analysis of parent cells and its transfectants. Thymosin-β4 at 295 bp in sense thymosin-β4 transfectants was increased, whereas it was reduced in antisense thymosin-β4 transfectants. **A:** QR-32 cells transfected with sense thymosin-β4 construct. **B:** QRsP-30 cells transfected with antisense thymosin-β4 construct.

thymosin-β4 levels in the sense or antisense cDNA transfected cells was caused by the transfected thymosin-β4 gene instead of the transfection procedures, ie, vector construct or neomycin selection.

We then confirmed the expression of thymosin-β4 protein by Western blotting. To make sure that the monoclonal antibody used in this study was specific to thymosin-β4, we performed two experiments: competitive inhibition assay and Western blot analysis by using synthetic β-thymosin-peptides. The competitive inhibition curves obtained from the reaction with the antibody raised against the synthetic peptide of thymosin-β4 or thymosin-β10 demonstrated practically no cross-reactivity with thymosin-β10 (Figure 3A). For confirming the specificity of the antibody, the synthetic full-size peptide of thymosin-β4 and thymosin-β10 were electrophoresed and the gel was stained with Coomassie brilliant blue solution (Figure 3B). The peptides in another gel were transferred onto membrane and incubated with thymosin-β4 (TB4N1-5) monoclonal antibody (1 μg/ml). Figure 3C shows TB4N1-5 monoclonal antibody reacts with thymosin-β4 peptide but not thymosin-β10. When the thymosin-β4 antibody was preabsorbed with the purified thymosin-β4, the intensity of the signal markedly decreased (data not shown).

The results obtained by RT-PCR were also confirmed by Western blotting analysis using the specific thymosin-β4 antibody. Thymosin-β4 protein was detected as a single band of 7.6 kd in 32-S cells transfected with sense thymosin-β4 cDNA but very faint bands were detected in the samples obtained from QR-32 cells and its vector control transfectants (Figure 4A). Thymosin-β4 protein was detected in QRsP-30 cells and its vector control transfectants; however, the samples obtained from QRsP-30 cells transfected with antisense thymosin-β4 cDNA revealed declined thymosin-β4 levels (Figure 4B).

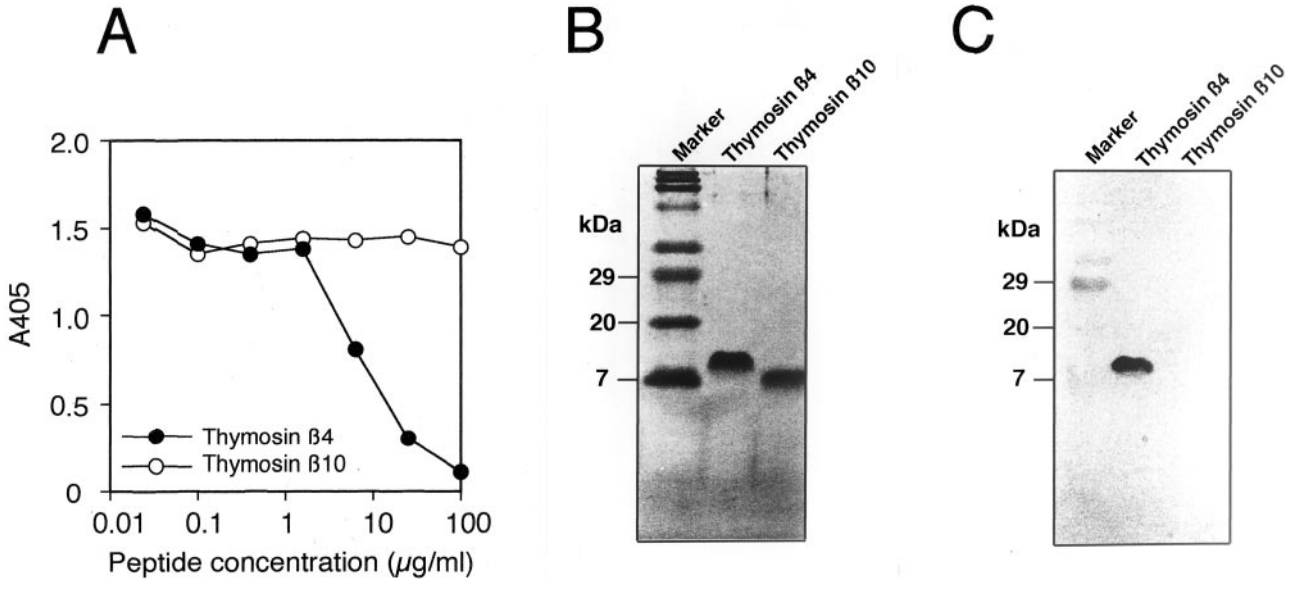

Figure 3. Specificity of the monoclonal antibody, TB4N1-5, as determined by Western blot and competitive inhibition assay. **A:** Peptide competitive inhibition assay. The 96-well plates were precoated with synthetic peptide of thymosin-β4 (2 μg/ml). TB4N1-5 antibody (5 μg/ml) was added to the wells with serially diluted synthetic peptide, thymosin-β4 (●) or thymosin-β10 (○). Absorbance at 405 nm was measured after incubation with ABTS and HRP-conjugated anti-mouse immunoglobulins as described in Materials and Methods. **B:** Coomassie brilliant blue staining. The synthetic peptides of thymosin-β4 and thymosin-β10 (1.5 μg/lane) were electrophoresed in SDS-polyacrylamide gel electrophoresis and the gel was stained with Coomassie brilliant blue solution. **C:** Western blotting by TB4N1-5 antibody. Another gel, electrophoresed as the same procedures as described in **A**, were transferred onto membrane and reacted with TB4N1-5 antibody (1 μg/ml).

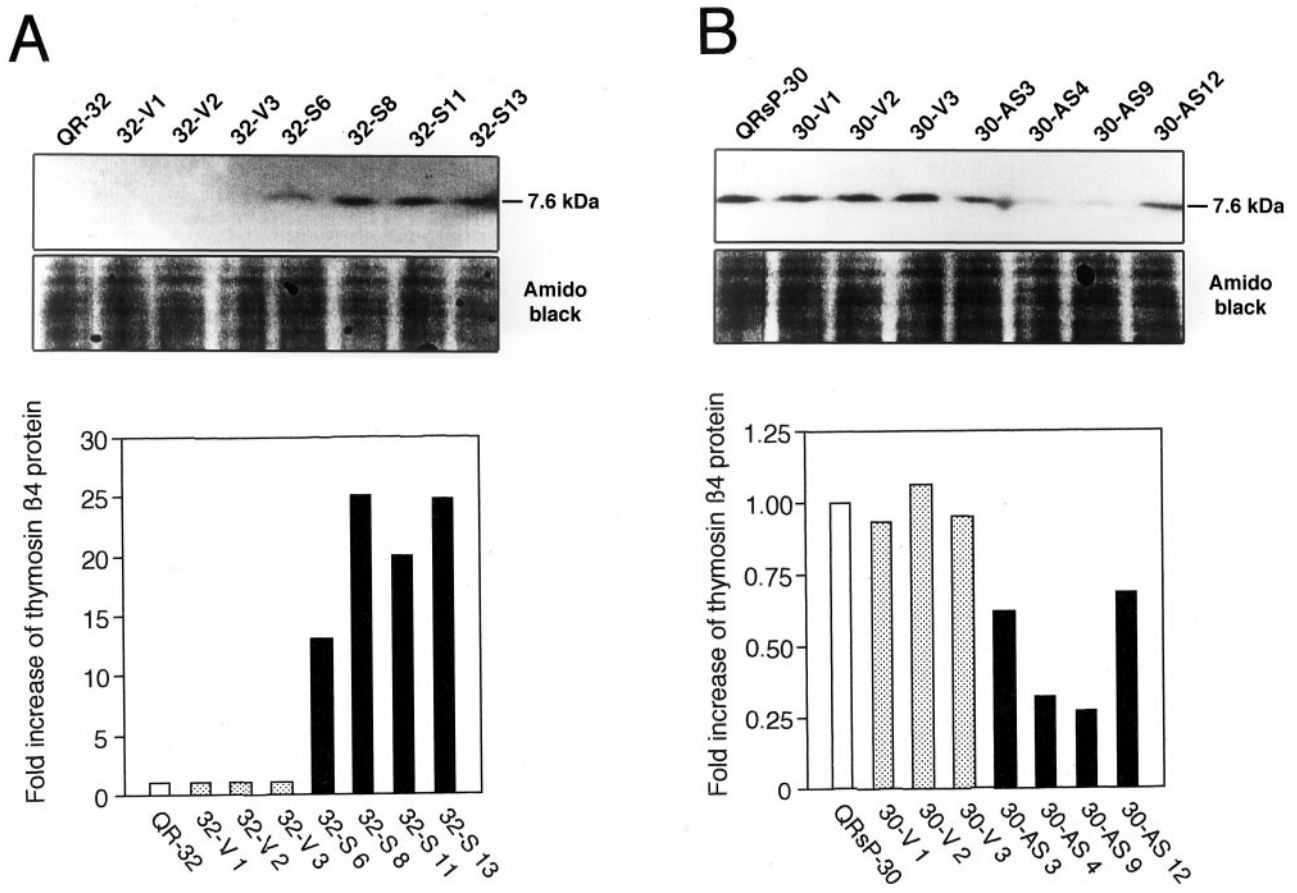

Figure 4. Western blot of thymosin-β4 protein levels in the cells transfected with sense or antisense thymosin-β4 construct and vector controls. Western blot analysis of parent cells and its transfectants. Thymosin-β4 (Mr 7600) in sense thymosin-β4 transfectants was increased, whereas it was reduced in antisense thymosin-β4 transfectants. The expression of thymosin-β4 proteins comparing Amido Black staining were quantified by densitometry. **A:** QR-32 cells transfected with sense thymosin-β4 construct. **B:** QRsP-30 cells transfected with antisense thymosin-β4 construct.

In vitro growth characteristics of the transfected cells had some clonal variations but were very similar to those of empty vector-transfected controls and parental non-transfected cells except for plating efficiency (Table 1).

Metastatic Ability of Tumor Cells Associated with Thymosin-β4 Expression

We evaluated the metastatic ability of the transfectants (Table 2). None of the QR-32 cells or 32-V clones, except the 32-V1 clone, metastasized to lung after intravenous injection into C57BL/6 mice. In contrast, 32-S clones developed lung metastatic nodules and significantly increased incidences of lung metastasis. Two of four 32-S clones metastasized to other organs such as ovary or peritoneal cavity. In contrast, QRsP-30 and 30-V clones aggressively metastasized to the lungs, ovaries, and peritoneal cavities; however, antisense thymosin-β4 cDNA-transfected clones, 30-AS4 and 30-AS9, had significantly less lung colonization and none of the 30-AS clones had metastasis in other organs. Under similar conditions, the mean survival periods of 30-AS clone-injected mice were significantly longer than those of QRsP-30 or 30-V clone-injected mice (60.2 ± 12.0 *versus*

Table 1. *In Vitro* Characteristics of Sense or Antisense Thymosin-β4-Transfected Mouse Fibrosarcomas

Cells	Doubling time (hour)	Plating efficiency (%)*	Colony formation in soft agar (%)†
QR-32	21.8	49.3 ± 4.1	40.0
32-V1	20.7	51.6 ± 2.0	47.3
32-V2	25.6	52.6 ± 2.0	45.0
32-V3	25.8	51.1 ± 2.2	49.3
32-S6	28.0	58.6 ± 1.0‡	50.0
32-S8	22.8	65.5 ± 2.3‡	48.3
32-S11	28.0	64.5 ± 3.5‡	41.3
32-S13	26.8	64.5 ± 1.8‡	44.0
QRsP-30	24.0	61.5 ± 2.2	32.7
30-V1	24.3	58.1 ± 4.2	41.7
30-V2	24.9	61.6 ± 3.1	36.0
30-V3	21.4	60.5 ± 1.8	35.7
30-AS3	42.0	44.0 ± 1.8§	26.0
30-AS4	25.9	50.3 ± 3.0¶	30.0
30-AS9	27.7	51.8 ± 3.3‖	33.0
30-AS12	35.4	50.3 ± 2.2¶	31.3

*One × 10^3 cells of each cell line were plated into 60-mm dishes and incubated for 7 days.

†Two × 10^2 cells were suspended in 1 ml of 0.3% agar and plated on a presolidified 0.6% agar in 6-well plates and incubated for 3 weeks.

‡$P < 0.001$ *versus* 32-V2 cells.

§$P < 0.001$; ¶$P < 0.005$, ‖$P < 0.05$ *versus* 30-V1 cells.

Table 2. Experimental Metastatic Ability of Sense or Antisense Thymosin-β_4 Transfectants and Their Control Cell Lines

	Intravenous injections*							
	Lung colonizing ability†				Other metastasized organs††			
	Incidence (no. of mice with lung metastasis/no. of mice tested)				Incidence (no. of mice with metastases/no. of mice tested)			
Cells	Exp. I	Exp. II	Total	No. of lung metastatic nodules**	Exp. I	Exp. II	Total	Sites (incidence)
QR-32	0/5	0/5	0/10	0,0,0,0,0,0,0,0,0,0	0/5	0/5	0/10	No metastases
32-V1	1/5	0/5	1/10¶	0,0,0,0,0,0,0,0,0,25	0/5	0/5	0/10	No metastases
32-V2	0/5	0/5	0/10¶	0,0,0,0,0,0,0,0,0,0	0/5	0/5	0/10	No metastases
32-V3	0/5	0/5	0/10¶	0,0,0,0,0,0,0,0,0,0	0/5	0/5	0/10	No metastases
32-S6	2/5	4/5	6/10§	0,0,0,0,18,21,21,26,28,31	0/5	0/5	0/10	No metastases
32-S8	4/5	3/5	7/10§	0,0,0,11,19,22,25,26,30,32	1/5	2/5	3/10	Ascites(2/10), ovary(1/10)
32-S11	5/5	5/5	10/10¶	6,6,7,8,12,17,18,18,21,43	1/5	0/5	1/10	Ascites, ovary(1/10)
32-S13	3/5	4/5	7/10§	0,0,0,18,18,21,29,32,32,34	0/5	0/5	0/10	No metastases
QRsP-30	4/5	5/5	9/10	0,9,11,12,18,30,44,>150,>150,>150	1/5	2/5	3/10	Ascites(2/10), ovary(2/10)
30-V1	4/5	5/5	9/10‖	0,9,13,17,25,40,>150,>150,>150,>150	0/5	2/5	2/10	Ascites(2/10), ovary(1/10)
30-V2	4/5	5/5	9/10‖	0,3,5,16,18,27,30,46,>150,>150	2/5	0/5	2/10	Ascites, ovary(1/10), ovary(1/10)
30-V3	3/5	5/5	8/10‖	0,0,5,5,11,15,15,19,25,>150	1/5	1/5	2/10	Ascites(2/10), ovary(1/10)
30-AS3	4/5	3/5	7/10‖	0,0,0,5,9,9,12,17,18,20	0/5	0/5	0/10	No metastases
30-AS4	2/5	2/5	4/10‡	0,0,0,0,0,0,5,6,12,27	0/5	0/5	0/10	No metastases
30-AS9	2/5	2/5	4/10‡	0,0,0,0,0,0,8,9,12,28	0/5	0/5	0/10	No metastases
30-AS12	5/5	2/5	7/10‖	0,0,0,2,3,9,18,30,38,>150	0/5	0/5	0/10	No metastases

*One $\times$ 10^6 cells of each line were intravenous injected into mice.
†Twenty-five days later, the mice were sacrificed and the metastatic nodules on the lung surface were counted macroscopically.
The incidence of lung metastasis: ‡P <0.05; §P <0.005; ¶P <0.001; ‖not significant *versus* original tumor cells.
**Each value represents the number of colonies per mouse lung.
††Other organ metastases were also examined macroscopically.

45.1 ± 12.5 or 49.1 ± 10.4 days, respectively, $P <$ 0.001).

We next evaluated the tumor-forming ability of the transfectants (Table 3). None of the QR-32 cells or empty vector-transfected clones (32-V1, 32-V2, and 32-V3) formed tumors; in contrast, 32-S clones that overexpressed thymosin-β4 formed lethal tumors in the mice. On the other hand, all of the QRsP-30 cells and the 30-V clones were found to form subcutaneous tumors and to develop spontaneous metastases to the lungs. The inci-

Table 3. Subcutaneous Tumorigenicity and Spontaneous Lung Metastatic Ability of Sense or Antisense Thymosin-β_4 Transfectants and Their Control Cell Lines

	Subcutaneous tumorigenicity*					Spontaneous metastasis†			
	Incidence (no. of tumors/no. of mice tested)			Latency periods (days)	Mean survival time (days)	Incidence (no. of mice with lung metastasis/no. of mice tested)			No. of colonies per mouse lung‖
Cells	Exp. I	Exp. II	Total			Exp. I	Exp. II	Total	
QR-32	0/5	0/5	0/10	Alive	Alive	0/5	0/5	0/10	0,0,0,0,0,0,0,0,0,0
32-V1	0/5	0/5	0/10¶	Alive	Alive	0/5	0/5	0/10¶	0,0,0,0,0,0,0,0,0,0
32-V2	0/5	0/5	0/10¶	Alive	Alive	0/5	0/5	0/10¶	0,0,0,0,0,0,0,0,0,0
32-V3	0/5	0/5	0/10¶	Alive	Alive	0/5	0/5	0/10¶	0,0,0,0,0,0,0,0,0,0
32-S6	1/5	0/5	1/10¶	20	68	0/5	0/5	0/10¶	0,0,0,0,0,0,0,0,0,0
32-S8	1/5	1/5	2/10¶	15,18	57,63	0/5	0/5	0/10¶	0,0,0,0,0,0,0,0,0,0
32-S11	1/5	0/5	1/10¶	13	51	1/5	0/5	1/10¶	0,0,0,0,0,0,0,0,0,3
32-S13	1/5	0/5	1/10¶	15	73	0/5	0/5	0/10¶	0,0,0,0,0,0,0,0,0,0
QRsP-30	5/5	5/5	10/10	11.2 ± 1.5	31.2 ± 5.0	2/5	4/5	6/10	0,0,0,0,2,3,5,5,8,10
30-V1	4/4	5/5	9/9¶	13.4 ± 5.3§§	33.7 ± 6.6§§	1/4	2/5	3/9¶	0,0,0,0,0,0,2,2,6
30-V2	4/4	5/5	9/9¶	12.8 ± 5.8§§	33.8 ± 10.4§§	2/4	2/5	4/9¶	0,0,0,0,0,2,2,2,5
30-V3	5/5	5/5	10/10¶	10.0 ± 0.0§§	32.2 ± 3.0§§	1/5	3/5	4/10¶	0,0,0,0,0,0,2,2,4,6
30-AS3	2/5	2/5	4/10§	20.8 ± 7.8‡‡	41.3 ± 10.1††	0/5	0/5	0/10§	0,0,0,0,0,0,0,0,0,0
30-AS4	5/5	4/5	9/10¶	16.2 ± 4.4**	38.6 ± 12.3§§	2/5	1/5	3/10¶	0,0,0,0,0,0,0,2,2,4
30-AS9	4/5	5/5	9/10¶	13.4 ± 2.2††	32.8 ± 8.1§§	0/5	0/5	0/10§	0,0,0,0,0,0,0,0,0,0
30-AS12	2/5	3/5	5/10‡	17.0 ± 7.8††	40.0 ± 5.5‡‡	0/5	0/5	0/10§	0,0,0,0,0,0,0,0,0,0

*Two $\times$ 10^5 cells from either transfected cells or the original tumor cells were injected subcutaneous into normal C57BL/6 mice.
†The tumor-bearing mice were sacrificed and autopsied when they were moribund. The metastatic nodules on the lung surface were counted macroscopically.
Tumorigenicity and lung metastasis of all the cell lines: ‡P <0.01; §P <0.005; ¶not significant *versus* original tumor cells.
‖Each value represents the number of colonies per mouse lung.
Mean latency periods or mean survival days: **P <0.01; ††P <0.05; ‡‡P <0.005; §§not significant *versus* original tumor cells.

dence of tumor formation was decreased in the 30-AS3 and 30-AS12 cells and all of the 30-AS cells had significantly prolonged latency periods as compared to the parental tumor cells. Moreover, three of four 30-AS cells significantly reduced the incidence of spontaneous metastasis to the lungs at autopsy.

The metastatic ability, as well as tumorigenic potential, was more likely to correlate in proportion to the protein levels of thymosin-β4 in the transfectants.

Thymosin-β4 Expression and in Vitro *Tumor Cell Motility*

The motility of thymosin-β4 transfectants and their control cells was examined using two separate assays. We used phagokinetic track assay to examine motile potential of single cells. The mean motility of 32-S clones was $57.1 \pm 7.5 \times 10^3$ μm^2, which was ~3.6-fold greater than that the mean values of 15.9 ± 1.0 μm^2 determined in the 32-V clones (Figure 5A). The motility of QRsP-30 cells was 5.2-fold greater than that of the parental QR-32 cells; however, 30-AS clones were less motile than 30-V clones: $47.1 \pm 5.8 \times 10^3$ μm^2 *versus* $88.5 \pm 1.1 \times 10^3$ μm^2 (Figure 5B).

We next confirmed cell motility phenotype by scratch-wound closure assay, which reveals potential of the cells for dissociation from closely attached cell population and cell motile phenotype. The numbers of the cells that moved into the scratched area after 12 hours were counted in a microscope. Figure 5, C and D, showed that motile potential of 32-S clones into the scratched area was significantly increased compared to QR-32 cells and 32-V clones (Figure 5C, $P < 0.005$). QRsP-30 tumor cells was approximately threefold more motile into the scratched area than QR-32 cells. 30-AS clones were significantly reduced motile potential as compared to QRsP-30 and 30-V clones (Figure 5D, $P < 0.001$).

These results demonstrated that level of thymosin-β4 expression is associated with cell motility, suggesting that thymosin-β4 may regulate metastasis by controlling cytoskeletal alterations essential for cell motility.

Thymosin-β4 Expression and Actin-Based Cytoskeletal Organization

We next examined thymosin-β4 expression by immunofluorescence staining with anti-thymosin-β4 antibody (green) and actin-based cytoskeletal changes by Texas Red-X phalloidin staining (red) using confocal microscopy. Thymosin-β4 expression was observed mainly in the cytoplasm of the cells that was coincident with the previous reports.[17,18] Low expression of thymosin-β4 in 32-V and 30-AS clones have strong F-actin staining at the cytoskeleton (Figure 6), however, high expression of thymosin-β4 in 32-S and 30-V have weak and irregular staining. Sensitive confocal laser sectioning and subsequent computer-assisted image merging revealed that thymosin-β4 partially merged with F-actin but thymosin-β4 mainly localized at the cytoplasm, whereas F-actin localized at the cytoskeleton (Figure 6).

The most profound change in thymosin-β4 transfectants was an alteration of cell shape. Increased thymosin-β4 expression could induce morphological change in QR-32 cells, which are larger, ie, elongated, spread, spindle-shaped, and have less F-actin staining similar to that QRsP-30 tumor cells, whereas antisense thymosin-β4 transfected cells reversed morphological change in QRsP-30 cells similar to that of QR-32 cells (Figure 6). These morphological changes were consistently observed in all of the transfected clones expressing thymosin-β4 but not in those transfected with an empty vector.

Discussion

In the present study, we found that expression of thymosin-β4 was enhanced in all of the highly metastatic cell lines converted from parental nonmetastatic fibrosarcoma cell clone. Also we demonstrated that the thymosin-β4 molecule acted as a positive regulator of cell motility through actin-based cytoskeletal organization by sense or antisense cDNA transfection. From these, we confirmed that thymosin-β4 regulates tumorigenicity and metastasis of tumor cells.

β-thymosins are a family of small peptides that were originally supposed to be thymic hormone.[19] They were then identified as actin monomer-binding proteins[20,21] that bind monomeric actin (G-actin) and disturb the assembly of filamentous actin (F-actin).[22,23] The balance of those two types of actins maintains the cytoskeletal actin for polymerization.[19,20] Among β-thymosin members, thymosin-β4 has been the most thoroughly studied, which is expressed ubiquitously in mammalian cells.[24,25]

Enhanced thymosin-β4 expression is observed in medullary thyroid carcinoma[26] and renal tumor[27] as compared with their normal counterparts. Clark and colleagues[28] have recently reported that thymosin-β4 is involved in the formation of metastasis of both human and mouse melanoma cells from their analysis by DNA array. We found that thymosin-β4 was highly expressed in the tumor cells progressed from weakly tumorigenic and nonmetastatic fibrosarcoma cells and that the expression regulated not only tumorigenicity but metastatic ability of the tumor cells that is facilitated through cell motility. Stimulation of cell motility phenotype is a common feature of β-thymosins as seen in thymosin-β10[29] and thymosin-β15.[30] It was also reported that those β-thymosins are expressed in advanced tumors and highly metastatic human tumor cells.[30–34] Namely, increased cell motility is associated with enhanced metastatic potential of animal and human tumors.[35,36]

Interestingly, we found that thymosin-β4 expression regulated plating efficiency, whereas *in vitro* cell growth or ability of colony formation was not associated with thymosin-β4 expression (Table 1). These results may indicate that thymosin-β4 regulates cell attachment to substrate and spreading. Figure 4 shows that dramatic morphological alteration followed thymosin-β4 expression. The thymosin-β4-induced morphological change is

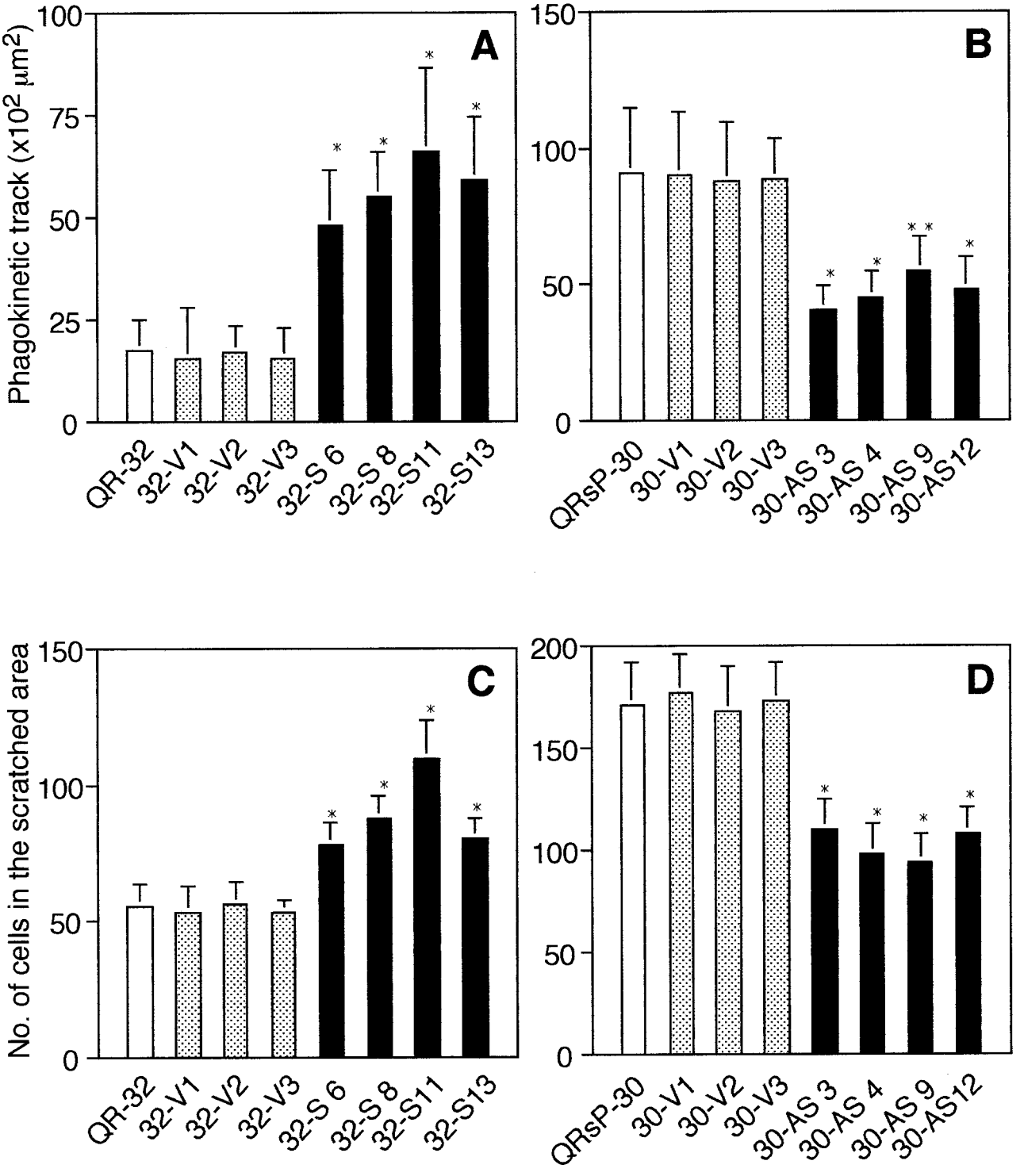

Figure 5. Phagokinetic track patterns produced by sense (**A**) or antisense (**B**) thymosin-β4 transfectants and their control tumor cells. The gold particles were scattered on the glass coverslips. Tumor cells were plated on the glass coverslips in culture. After 48 hours of incubation, the phagokinetic track areas of 40 individual cells were measured and the average area is shown. Each bar represents the means ± SD of three independent experiments done in duplicate. *, $P < 0.001$; **, $P < 0.005$, compared with an empty-vector transfectant. Scratch-wound closure patterns produced by sense (**C**) or antisense (**D**) thymosin-β4 transfectants and their control tumor cells. An *in vitro* wound was introduced in confluent cultures of each cell lines. After 12 hours, the cells were photographed. The number of cells migrated into the scratched area was counted. Each bar represents the means ± SD of three independent experiments done in duplicate. *, $P < 0.001$, compared with an empty-vector transfectant.

quite similar to what is referred as epithelial-to-mesenchymal transition (EMT). It has been suggested that EMT occurs in many developmental systems and tumor metastasis, and that it is triggered by balanced cross-modulation among cell-cell adhesion molecules (such as E- or N-cadherins), cell-ECM adhesion molecules, and actin-based cytoskeletal molecules. On the basis of our results and other researchers,[37,38] we suggested that increased

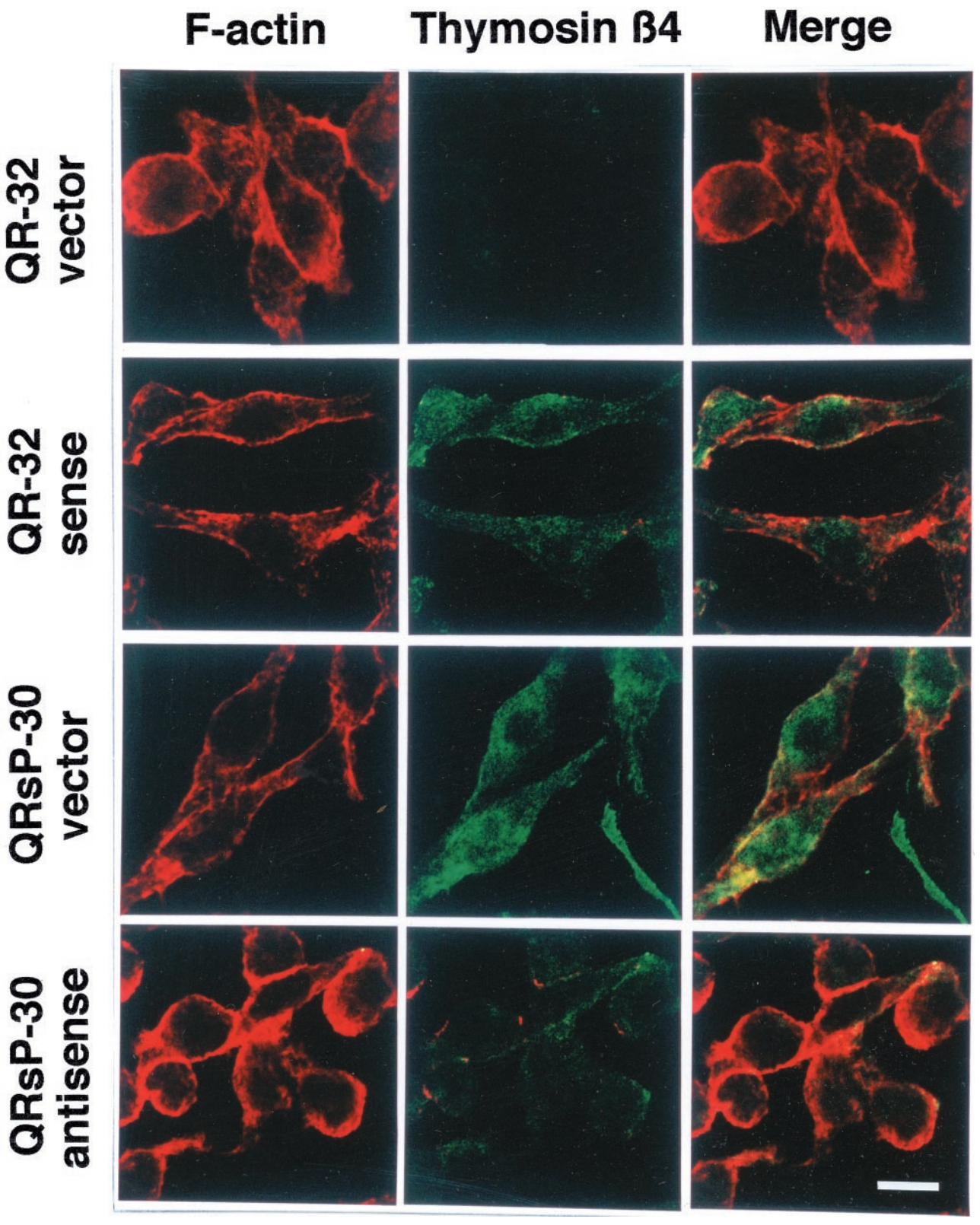

Figure 6. Thymosin-β4 levels inversely correlates with F-actin staining. Benign or malignant mouse fibrosarcoma cells expressing vector construct, and sense and antisense thymosin-β4 cDNA has been attached onto glass coverslips, then fixed and stained with thymosin-β4 antibody (green) and Texas Red-X phalloidin (red) to detect thymosin-β4 distribution and F-actin, respectively, and observed by confocal scanning laser microscopy. Original magnification of each clone, ×630. Representative image of three independent experiments with similar results is shown. Scale bar, 10 μm.

adhesion, spreading, and EMT-like morphological changes could be because of the downstream effects of the increased thymosin-β4.

Significant progress has been made recently in identifying and clarifying the roles of thymosin-β4. It is known that thymosin-β4 is involved in the regulation of actin-based cytoskeleton and focal adhesion proteins that are localized to the termini of the stress fiber-like actin filaments, as well as in the cell-cell junctions adjacent to circumferential actin bundles.[39] Thymosin-β4 induces myosin IIA, α-actinin, and tropomyosin expressions that are known to compose stress fibers or the actin bundles,[38,40,41] also, it has been shown to induce focal adhesion proteins such as vinculin, talin, α_5-integrin, focal adhesion kinase (pp^{125}FAK),[38,40,41] and possibly to cross-link to p130 Crk-associated substrate (Cas) and paxillin.[42–45] Both thymosin-β4[46] and actin[47] serve as an endogenous substrate for transglutaminases; therefore, the thymosin-β4 seems to play an important role in transglutaminase-related apoptotic processes *in vivo*. Niu and Nachmias[42] have reported that enhanced thymosin-β4 gene expression induced resistance to ultraviolet or TNF-α-induced apoptosis in NIH3T3 cells, which was dependent on the phosphorylation of focal adhesion kinase (pp^{125}FAK) and its-associated actin cytoskeleton-associated protein, paxillin.[48] Taken together, escape from physiologically induced apoptosis *in vivo* will be an important factor for survival of malignant tumor cells. Furthermore, thymosin-β4 stimulates angiogenesis,[49,50] wound healing,[51] and blood coagulation;[20,52] all of these are critical for tumor cells to acquire metastatic phenotype. Reorganization of the actin network by thymosin-β4 expression may therefore affect the dynamics of focal adhesion assembly and lead to modulation of cell-substratum interaction, cellular shape, cell motility, cell survival, and consequently metastatic ability of tumor cells.

The expression of thymosin-β4 after malignant progression of mouse fibrosarcoma cells differed depending on the causes of progression. All of the malignant fibrosarcoma cell lines used in this study, converted from QR-32 cells by inflammation induced at the implantation site, expressed high levels of thymosin-β4 mRNA. We have recently established an *in vivo* model of tumor progression in which the QR-32 cells acquire malignant phenotype by administration of antitumor drugs, such as adriamycin,[9] *cis*-diaminedichloro-platinum (II) (cisplatin), or UFT.[10] Such antitumor drug-induced malignant tumor cell lines express only a slight increase of thymosin-β4 mRNA expression (less than threefold as compared to QR-32 cells, data not shown). We observed that activated leukocyte cell adhesion molecule and annexin II genes were expressed in the antitumor drug-induced malignant tumors cells and that they controlled their metastatic potential.[8] Those results indicate the gene expression associated with malignant conversion of QR-32 cells strictly differ depending on the causes of progression.

The correlation between thymosin-β4 expression and tumor malignancy does not seem to be a common phenomenon in all of the organs. Yamamoto and colleagues[53] showed an inverse relation between thymosin-β4 expression and the liver metastatic ability of human colorectal carcinoma cells. There was no explanation in that work how the reduced expression of thymosin-β4 related with the promoted metastatic ability. An interpretation of the discrepancy is still unclear, however, several points need to be taken into account to clarify the role of thymosin-β4 in carcinogenesis and metastatic potential of tumors. Firstly, the organ environment and genetic alteration(s) affects the β-thymosin expression. We observed that the thymosin-β4 expression in the *in vivo* growing malignant tumor cells (Figure 1, C and D) was much higher than that of the thymosin-β4-transfected tumor cells (Figure 2A). We speculated that this phenomenon resulted from host selection pressure to allow highly thymosin-β4 expressed cells to grow. Another speculation was that the thymosin-β4 level can be altered rapidly by environmental stimuli.[54] A recent report has shown that oxidation also modulates the function of thymosin-β4; for instance, it attenuates G-actin sequestering activity.[55,56] Other studies have demonstrated that, tumor-suppressing maspin (mammary serine protease inhibitor) is one of the isoforms of serpin binding to thymosin-β4 as ligand[57] and that the maspin is regulated directly by the p53 tumor suppressor gene.[58] It is well known that p53 mutation in the colorectal tumors is accumulated at advanced phase; it is most likely that the environmental circumstances of the colorectal carcinoma (ie, oxidative stress induced by inflammation or bacterial microflora) may directly or indirectly modulate the function of the thymosin-β4. Secondly, in most studies only one type of β-thymosin has been investigated, although most cells and tissues express at least two or three β-thymosins that may share the same function(s). In the colon, the major β-thymosin may vary. Califano and colleagues[33] have observed that overexpression of thymosin-β10, which is another abundant β-thymosin in mammalian cells[24] with a high degree of sequence homology to thymosin-β4, in the neoplastic transformation of the colon epithelial cell.

To show tumorigenic and metastatic function of β-thymosins in relation with their G-actin sequestering activities, we need to determine the intracellular peptide concentration or changes in G-actin/F-actin ratio or identification of receptors for the peptide. Investigations at such standpoints of view will help us elucidate the role of β-thymosin in tumor development and progression, for which we are now undertaking experiments.

Acknowledgments

We thank Dr. Kazumi Goto at Niigata University for her helpful detailed suggestion to the procedure of Western blotting and Miss Masako Yanome for her help in the English revision of the manuscript.

References

1. Steeg PS, Bevilacqua G, Kopper L, Thorgeirsson UP, Talmadge JE, Liotta LA, Sobel ME: Evidence for a novel gene associated with low tumor metastatic potential. J Natl Cancer Inst 1988, 80:200–204
2. Lee J-H, Miele ME, Hicks DJ, Phillips KK, Trent JM, Weissman BE,

Welch DR: KiSS-1, a novel human malignant melanoma metastasis-suppressor gene. J Natl Cancer Inst 1996, 88:1731–1737
3. Ebralidze A, Tulchinsky E, Grigorian M, Afanasyeva A, Senin V, Revazova E, Lukanidin E: Isolation and characterization of a gene specifically expressed in different metastatic cells and whose deduced gene product has a high degree of homology to a Ca^{2+}-binding protein family. Genes Dev 1989, 3:1086–1093
4. Gunthert U, Hofmann M, Rudy W, Reber S, Zoller M, Haussmann I, Matzku S, Wenzel A, Ponta H, Herrlich P: A new variant of glycoprotein CD44 confers metastatic potential to rat carcinoma cells. Cell 1991, 65:13–24
5. Okada F, Hosokawa M, Hamada J-I, Hasegawa J, Koto M, Mizutani T, Ren J, Takeichi N, Kobayashi H: Malignant progression of a mouse fibrosarcoma by host cells reactive to a foreign body (gelatin sponge). Br J Cancer 1992, 66:635–639
6. Okada F, Hosokawa M, Hamada J, Hasegawa J, Mizutani M, Takeichi N, Kobayashi H: Progression of a weakly tumorigenic mouse fibrosarcoma at the site of early phase of inflammation caused by plastic plates. Jpn J Cancer Res 1993, 84:1230–1236
7. Okada F, Nakai K, Kobayashi T, Shibata T, Tagami S, Kawakami Y, Kitazawa T, Kominami R, Yoshimura S, Suzuki K, Taniguchi N, Inanami O, Kuwabara M, Kishida H, Nakae D, Konishi Y, Moriuchi T, Hosokawa M: Inflammatory cell-mediated tumour progression and minisatellite mutation correlate with the decrease of antioxidative enzymes in murine fibrosarcoma cells. Br J Cancer 1999, 79:377–385
8. Choi S, Kobayashi M, Wang J, Habelhah H, Okada F, Hamada J-I, Moriuchi T, Totsuka Y, Hosokawa M: Activated leukocyte cell adhesion molecule (ALCAM) and annexin II are involved in the metastatic progression of tumor cells after chemotherapy with Adriamycin. Clin Exp Metastasis 2000, 18:45–50
9. Hosokawa M, Nakai K, Okada F: Tumor progression accelerated by oxygen species and its chemoprevention. Food Factors for Cancer Prevention. Edited by H Ohigashi, T Osawa, J Terao, S Watanabe, T Yoshikawa. Tokyo, Springer-Verlag, 1997, pp 77–81
10. Choi S, Okada F, Kobayashi M, Habelhah H, Nakae D, Konishi Y, Totsuka Y, Hosokawa M: Single treatment with cisplatin or UFT, but not their combination treatment enhances the metastatic capacity of mouse fibrosarcoma cells. Anticancer Drugs 1999, 10:235–243
11. Okada F, Hosokawa M, Hasegawa J, Ishikawa M, Chiba I, Nakamura Y, Kobayashi H: Regression mechanisms of mouse fibrosarcoma cells after in vitro exposure to quercetin: diminution of tumorigenicity with a corresponding decrease in the production of prostaglandin E2. Cancer Immunol Immunother 1990, 31:358–364
12. Okada F, Hosokawa M, Hasegawa J, Kuramitsu Y, Nakai K, Yuan L, Lao H, Kobayashi H, Takeichi N: Enhancement of in vitro prostaglandin E2 production by mouse fibrosarcoma cells after co-culture with various anti-tumour effector cells. Br J Cancer 1994, 70:233–238
13. Liang P, Pardee AB: Differential display of eukaryotic messenger RNA by means of the polymerase chain reaction. Science 1992, 257:967–971
14. Habelhah H, Okada F, Kobayashi M, Nakai K, Choi S, Hamada J-I, Moriuchi T, Kaya M, Yoshida K, Fijinaga K, Hosokawa M: Increased E1AF expression in mouse fibrosarcoma promotes metastasis through induction of MT1-MMP expression. Oncogene 1999, 18: 1771–1776
15. Laemmli UK: Cleavage of structural proteins during the assembly of the head of bacteriophage T4. Nature 1970, 227:680–685
16. Shibata T, Kawano T, Nagayasu H, Okumura K, Arisue M, Hamada J, Takeichi N, Hosokawa M: Enhancing effects of epidermal growth factor on human squamous cell carcinoma motility and matrix degradation but not growth. Tumor Biol 1996, 17:168–175
17. Yu FX, Lin SC, Morrison-Bogorad M, Yin HL: Effects of thymosin β4 and thymosin β10 on actin structures in living cells. Cell Motil Cytoskeleton 1994, 27:13–25
18. McCormack SA, Ray RM, Blanner PM, Johnson LR: Polyamine depletion alters the relationship of F-actin, G-actin, and thymosin β4 in migrating IEC-6 cells. Am J Physiol 1999, 276:C459–C468
19. Low TL, Hu SK, Goldstein AL: Complete amino acid sequence of bovine thymosin beta 4: a thymic hormone that induces terminal deoxynucleotidyl transferase activity in thymocyte populations. Proc Natl Acad Sci USA 1981, 78:1162–1166
20. Cassimeris L, Safer D, Nachmias VT, Zigmons SH: Thymosin beta 4 sequesters the majority of G-actin in resting human polymorphonuclear leukocytes. J Cell Biol 1992, 119:1261–1270
21. Safer D, Nachmias VT: Beta thymosins as actin binding peptides. Bioessays 1994, 16:590
22. Yu FX, Lin SC, Morrison-Bogorad M, Atkinson MA, Yin HL: Thymosin beta 10 and thymosin beta 4 are both actin monomer sequestering proteins. J Biol Chem 1993, 268:502–509
23. Jean C, Rieger K, Blanchoin L, Carlier MF, Lenfant M, Pantaloni D: Interaction of G-actin with thymosin beta 4 and its variants thymosin beta 9 and thymosin beta met9. J Muscle Res Cell Motil 1994, 15:278–286
24. Shimamura R, Kudo J, Kondo H, Dohmen K, Gondo H, Okamura S, Ishibashi H, Niho Y: Expression of the thymosin beta 4 gene during differentiation of hematopoietic cells. Blood 1990, 76:977–984
25. Gondo H, Kudo J, White JW, Barr C, Selvanayagam P, Saunders GF: Differential expression of the human thymosin-beta-4 gene in lymphocytes, macrophages, and granulocytes. J Immunol 1987, 139:3840–3848
26. Conlon JM, Grimelius L, Wallin G, Thim L: Isolation and structural characterization of thymosin-beta 4 from a human medullary thyroid carcinoma. J Endocrinol 1988, 118:155–159
27. Hall AK: Differential expression of thymosin genes in human tumors and in the developing human kidney. Int J Cancer 1991, 48:672–677
28. Clark EA, Golub TR, Lander ES, Hynes RO: Genomic analysis of metastasis reveals an essential role for Rho C. Nature 2000, 406:532–535
29. Sun HQ, Kwiatkowska K, Yin HL: β-thymosins are not simple actin monomer buffering proteins. J Biol Chem 1996, 271:9223–9230
30. Bao L, Loda M, Janmey PA, Stewart R, Anand-Apte B, Zetter BR: Thymosin B15: a novel regulator of tumor motility upregulated in metastatic prostate cancer. Nat Med 1996, 2:1322–1328
31. Santelli G, Califano D, Chiappetta G, Vento MT, Bartoli PC, Zullo F, Trapasso F, Viglietto G, Fusco A: Thymosin beta-10 gene overexpression is a general event in human carcinogenesis. Am J Pathol 1999, 155:799–804
32. Gold JS, Bao L, Ghoussoub RA, Zetter BR, Rimm DL: Localization and quantitation of expression of the cell motility-related protein thymosin beta15 in human breast tissue. Mod Pathol 1997, 10:1106–1112
33. Califano D, Monaco C, Santelli G, Giuliano A, Veronese ML, Berlingieri MT, de Franciscis V, Berger N, Trapasso F, Santoro M, Viglietto G, Fusco A: Thymosin beta-10 gene overexpression correlated with the highly malignant neoplastic phenotype of transformed thyroid cells in vivo and in vitro. Cancer Res 1998, 58:823–828
34. Bao L, Loda M, Zetter BR: Thymosin beta15 expression in tumor cell lines with varying metastatic potential. Clin Exp Metastasis 1998, 16:227–233
35. Hosaka S, Suzuki M, Goto M, Sato H: Motility of rat ascites hepatoma cells, with reference to malignant characteristics in cancer metastasis. Gann 1978, 69:273–276
36. Haemmerli G, Strauli P: In vitro motility of cells from human epidermoid carcinomas. A study by phase-contrast and reflection-contrast cinematography. Int J Cancer 1981, 27:603–610
37. Goodall GJ, Morgan JI, Hopecker BL: Thymosin β4 in cultured mammalian cell lines. Arch Biochem Biophys 1983, 221:598–601
38. Golla R, Philp N, Safer D, Chintapalli J, Hoffman R, Collins L, Nachmias VT: Co-ordinate regulation of the cytoskeleton in 3T3 cells overexpressing thymosin-β4. Cell Motil Cytoskeleton 1997, 38:187–200
39. Jones JL, Royall JE, Critchley DR, Walker RA: Modulation of myoepithelial-associated α6β4 integrin in a breast cancer cell line alters invasive potential. Exp Cell Res 1997, 235:325–333
40. Johnson RP, Craig SW: F-actin binding site masked by the intramolecular association of vinculin head and tail domains. Nature 1995, 373:261–264
41. Gilmore AP, Burridge K: Regulation of vinculin binding to talin and actin by phosphtidyl-inositol-4-5-bisphosphate. Nature 1996, 381: 531–535
42. Niu M, Nachmias VT: Increased resistance to apoptosis in cells overexpressing thymosin beta four: a role for focal adhesion kinase pp^{125}FAK. Cell Adhes Commun 2000, 7:311–320
43. Leventhal PS, Shelden EA, Kim B, Feldman EL: Tyrosine phosphorylation of paxillin and focal adhesion kinase during insulin-like growth factor-I-stimulated lamellipodial advance. J Biol Chem 1997, 272: 5214–5218
44. Konstantopoulos N, Clark S: Insulin and insulin-like growth factor-1

stimulate dephosphorylation of paxillin in parallel with focal adhesion kinase. Biochem J 1996, 314:387–390
45. Baron V, Calleja V, Ferrari P, Alengrin F, von Obberghen E: p125^{FAK} focal adhesion kinase is a substrate for the insulin and insulin-like growth factor-I tyrosine kinase receptors. J Biol Chem 1998, 273: 7162–7168
46. Huff T, Ballweber E, Humeny A, Bonk T, Becker C, Muller CS, Mannherz HG, Hannappel E: Thymosin β4 serves as a glutaminyl substrate of transglutaminase. Labeling with fluorescent dansylcadaverine does not abolish interaction with G-actin. FEBS Lett 1999, 464:14–20
47. Nemes Jr Z, Adany R, Balazs M, Boross P, Fesus L: Identification of cytoplasmic actin as an abundant glutaminyl substrate for tissue transglutaminase in HL-60 and U937 cells undergoing apoptosis. J Biol Chem 1997, 272:20577–20583
48. Hall AK: Molecular interactions between G-actin, DNase I and the beta-thymosins in apoptosis: a hypothesis. Med Hypotheses 1994, 43:125–131
49. Grant DS, Kinsella JL, Kibbey MC, LaFlamme S, Burbelo PD, Goldstein AL, Kleinman HK: Matrigel induces thymosin beta 4 gene in differentiating endothelial cells. J Cell Sci 1995, 108:3685–3694
50. Malinda KM, Goldstein AL, Kleinman HK: Thymosin beta 4 stimulates directional migration of human umbilical vein endothelial cells. FASEB J 1997, 11:474–481
51. Frohm M, Gunne H, Bergman AC, Agerberth B, Bergman T, Boman A, Liden S, Jornvall H, Boman HG: Biochemical and antibacterial analysis of human wound and blister fluid. Eur J Biochem 1996, 237: 86–92
52. Nachmias VT, Cassimeris L, Golla R, Safer D: Thymosin beta 4 (T beta 4) in activated platelets. Eur J Cell Biol 1993, 61:314–320
53. Yamamoto T, Gotoh M, Kitajima M, Hirohashi S: Thymosin beta-4 expression is correlated with metastatic capacity of colorectal carcinomas. Biochem Biophys Res Commun 1993, 193:706–710
54. Huff T, Muller CS, Otto AM, Netzker R, Hannappel E: β-thymosins, small acidic peptides with multiple functions. Int J Biochem Cell Biol 2001, 33:205–220
55. Heintz D, Reichert A, Mihelic-Rapp M, Stoeva S, Voelter W, Faulstich H: The sulfoxide of thymosin beta 4 almost lacks the polymerization-inhibiting capacity for actin. Eur J Biochem 1994, 223:345–350
56. Young JD, Lawrence AJ, MacLean AG, Leung BP, McInnes IB, Canas B, Pappin DJ, Stevenson RD: Thymosin β4 sulfoxide is an anti-inflammatory agent generated by monocytes in the presence of glucocorticoids. Nat Med 1999, 5:1424–1427
57. Hopkins PC, Whisstock J: Function of maspin. Science 1994, 265: 1893–1894
58. Zou Z, Gao C, Nagaich AK, Connell T, Saito S, Moul JW, Seth P, Appella E, Srivastava S: p53 regulates the expression of the tumor suppressor gene maspin. J Biol Chem 2000, 275:6051–6054